RSC Advances

PAPER

View Article Online
View Journal | View Issue

Cite this: *RSC Adv.*, 2023, **13**, 32473

Antimicrobial and antiviral evaluation of compounds from *Holoptelea integrifolia*: *in silico* supported *in vitro* study†

Hala Sh. Mohammed,[a] Eman F. S. Taha,[*b] Fatma S. Mahrous,[a] Rehab Sabour,[c] Marwa M. Abdel-Aziz[d] and Lotfy D. Ismail[e]

Holoptelea integrifolia, also known as the Indian Elm Tree, has been used in Ayurvedic medicine for its medicinal properties. In this study, two biologically active metabolites, 5(6) dihydrostigmast 22en 3-*O*-β-glucoside (DHS) and 1-*O*-eicosanoyl glycerol-2′-*O*-β-galactouronic (EGG), were isolated for the first time from the *n*-butanol fraction of *H. integrifolia* using a chromatographic technique and identified by NMR, and HRESI-MS. The antiviral and multidrug-resistant activities of these metabolites were evaluated as well as the *n*-butanol fraction. The *n*-butanol fraction of *H. integrifolia* exhibited weak antiviral effects, but DHS and EGG demonstrated significant antiviral activity against herpes simplex type-1 (HSV-1) and Coxsackie (CoxB4) viruses. Both metabolites showed lower IC_{50} values than the standard antiviral drug acyclovir, indicating their potency in inhibiting viral replication. EGG showed potent antiviral activity with minimal cytotoxicity at the highest concentration tested, presenting a selectivity index (SI) of 18.18 and 15.58 against HSV-1 and CoxB4 viruses, respectively. A preliminary assessment of the antibacterial activity of the *n*-butanol fraction and metabolites revealed that DHS had the highest inhibitory potency against drug-resistant strains, including MRSA and Carbapenem-resistant *Klebsiella pneumonia*. It also exhibited significant inhibitions against Fluconazole-resistant *Candida albicans* and ESBL – *Escherichia coli*. DHS displayed the lowest minimum inhibitory concentration (MIC) values, indicating its superiority as an antibacterial agent compared to EGG and the *n*-butanol fraction. Molecular docking analysis confirmed the antiviral and antibacterial actions of DHS and EGG by demonstrating their strong binding.

Received 2nd September 2023
Accepted 29th October 2023

DOI: 10.1039/d3ra05978b

rsc.li/rsc-advances

Introduction

Plant species are a valuable source of cost-effective and low-risk anti-infective medicines. The use of medicinal plants and traditional health systems is increasingly emphasized to address global healthcare concerns.[1–4] Traditional medical practices are considered an essential part of the culture in many emerging countries. *Holoptelea integrifolia*, or the Indian Elm Tree, is a large deciduous tree found throughout India up to an elevation of 2000 feet. Its bark is dark, pustular, and flakes in slightly corky scales.[5] The Ulmaceae family comprises 200 species divided into 15 genera found in tropical temperate areas of the Northern Hemisphere. Indian Elm grows up to 18 meters tall and has grey bark coated with blisters that flake in corky scales on older trees. Its leaves are elliptic-ovate, 8–13 cm long, and 3.2–6.3 cm broad, smooth, with whole edges and sharp points, and alternately placed. The base of the leaf is rounded or heart-shaped, and the stipules are lance-shaped. Crushed leaves emit a foul odor. The flowers are small, greenish yellow to brownish, hairy, and borne in short racemes or fascicles near leaf scars. The sepals are silky and usually four in number. The fruit is a 2.5 cm diameter circular samara with net-veined wings and flat seeds.[6] A literature review of the phytoconstituents of Indian Elm (*Holoptelea integrifolia*) revealed that it contains a variety of chemical compounds, including terpenoids, sterols, saponins, tannins, polysaccharides, proteins, flavonoids, and alkaloids. Additionally, 2-aminonaphthoquinone, friedelin, β-sitosterol, and β-D-glucose have been isolated from the stem bark of *H. integrifolia*. Lauric, myristic, palmitic, stearic, arachidic, behenic, hexadecenoic, and oleic acids were also found in the stem bark.[7] The leaves of the Indian Elm Tree contain friedelin or friedelin-type chemicals, which are effective in treating bladder cancer, convulsions, inflammation, topical

[a]*Department of Pharmacognosy and Medicinal Plants, Faculty of Pharmacy (Girls), Al-Azhar University, Cairo (11311), Egypt*

[b]*Department of Health Radiation Research, National Centre for Radiation Research and Technology, Egyptian Atomic Energy Authority (EAEA), Cairo, Egypt. E-mail: emanfayezsaid@gmail.com; Eman.Fayez@eaea.org.eg*

[c]*Department of Pharmaceutical Medicinal Chemistry and Drug Design, Faculty of Pharmacy (Girls), Al-Azhar University, Cairo, Egypt*

[d]*The Regional Centre for Mycology and Biotechnology, Al-Azhar University, Cairo, Egypt*

[e]*Department of Pharmacognosy and Medicinal Plants, Faculty of Pharmacy (Boys), Al-Azhar University, Cairo, Egypt*

† Electronic supplementary information (ESI) available. See DOI: https://doi.org/10.1039/d3ra05978b

ulcers, rheumatic inflammation, fever, and dysentery.[5,8] The leaves also contain hexacosanol, octacosanol, β-sitosterol, and β-amyrin. The heartwood has yielded β-sitosterol, 2,3-dihydroxyoelan-12-en-28-oic acid, and hederagenin.[9] *H. integrifolia* has traditionally been used to treat a variety of ailments, including inflammation, gastritis, dyspepsia, colic, intestinal worms, vomiting, wound healing, leprosy, diabetes, hemorrhoids, dysmenorrhea, and rheumatism.[10] The bark and leaves are bitter, astringent, thermogenic, anti-inflammatory, digestive, carminative, and laxative.[9] Stigmasterol glycosides are a type of saponin that exhibits a range of biological activities such as cytotoxicity and anti-inflammation.[11] Saponins exhibit a large range of biological activities, including cytotoxic, anti-inflammatory, hemolytic, antifungal, and antibacterial properties. Eicosanoyl glycerol is a fatty acid glycerol ester that has been shown to have antiviral properties.[12] For example, medium-chain fatty acids (MCFA) and glycerol monolaurate (GML) can inhibit the African swine fever virus (ASFv) in liquid and feed conditions.[13]

Butanol fraction of plants has garnered significant interest in the field of ethnopharmacology and natural product research. This fraction, obtained through solvent extraction, contains a diverse array of bioactive compounds with potential therapeutic applications. Studies have shown that the butanol fraction of plants possesses various pharmacological properties, including antioxidant, anti-inflammatory, and anticancer activities. For instance, research published in 2014 demonstrated the antioxidant potential of the butanol fraction of certain plants.[14] Additionally, the studies highlighted the anti-inflammatory effects of the butanol fraction in experimental models.[15] Moreover, Sunil *et al.* reported on the antimicrobial properties of the butanol fraction in food preservation.[16] Furthermore, Chang *et al.* showcased the anticancer potential of the butanol fraction in preclinical studies.[17] These studies collectively underscore the importance and versatility of the butanol fraction of plants as a valuable source of bioactive compounds for further exploration and development." Despite the abundance of literature on the leaves of *Holoptelea integrifolia*, its antiviral and antimicrobial activity remains largely unexplored. Our study aims to evaluate the antiviral activity of the *n*-butanol fraction of *H. integrifolia* leaves and isolated metabolites against Coxsackie Virus (CoxB4) and Herpes Simplex Virus Type I (HSV-I) in comparison to acyclovir, the reference antiviral drug. Additionally, we aim to assess the potential of multidrug resistance against antibiotic-resistant pathogens. This objective is supported by a comprehensive *in silico* modeling study.

Results and discussion

Phytochemistry

Metabolite 1. White amorphous powder (20 mg), based on chromatographic properties: R_f; 0.56 ethyl acetate : methanol (80 : 20 v/v), no fluorescence under UV light, on TLC provided pink spot with 10–15% ethanol/H_2SO_4 after heating at 120 °C, and affirmative to Liebermann's and Molisch's tests, predicted metabolite 1, as a steroid. The ^{1}H NMR spectrum (Table 1, Fig. S2†); showed presence of signals for two tertiary methyl groups at δ_H 0.62 (3H, s, Me-18), 1.03 (3H, s, Me-19); three secondary methyl groups at δ_H 0.98 (3H, d, $J = 6$ Hz, Me-21), 0.88 (3H, d, $J = 6.8$ Hz, Me-26), 0.79 (3H, d, $J = 6.8$ Hz, Me-27); one primary methyl group at δ_H 0.78 (3H, t, $J = 7.7$ Hz, Me-29), and that indicating the characteristic for stigmastane.[18,19] An additional functionality found included oxygenated proton at δ_H 3.96 (1H, m, H-3) and two olefinic methines at δ_H 5.15 (1H, dd, $J = 15.3$, 7.6 Hz, H-22) and 5.01 (1H, dd, $J = 15.3$, 7.6 Hz, H-23), which indicating for olefinic methine having trans position at C-22 and C-23. Twenty-nine carbon resonances were observed in the ^{13}C NMR spectrum (Table 1, Fig. S3†), these were assigned by DEPT-135 and HSQC (Fig. S4 and S5†) experiments to six methyls, ten sp^3 methylene, eight sp^3 methines, two quaternary carbons, two olefinic methines at δ_C 129.2 and 138.6, and one oxygenated methine carbon at δ_C 74.8. All previous data are characteristic of stigmastane-type steroid structure,[18,19] which was confirmed from the HMBC experiment (Fig. S6†). The HMBC spectra showed the correlation between the proton of methyl groups Me-18, 19, 21, 26, 27, and 29 with neighbor carbons supporting the presence of stigmastane type steroid in compound 1. The HMBC spectrum showed cross peaks of two olefinic methines from δ_C 129.2 (C-23) and 138.6 (C-22) to adjacent methin δ_H 1.91 (H-20) and 0.98(H-21) indicating olefinic methine was attached at C-22 and C-23. The hydroxy position in HMBC showed cross peaks at δ_H 1.72 (H-1) and 1.89 (H-2) to hydroxy methine δ_C 74.8 were indicated hydroxyl group at C-3, from above data confirmed aglycone as 5(6) dihydrostigmast 22en 3-ol,[18,19] and from chromatographic properties which showed R_f value at 0.56 confirmed the presence of metabolite 1 as a glycoside confirmed by the presence of anomeric proton of δ_H 4.16 (1H, d, $J = 7.8$ Hz, H-1′) and carbon resonance at δ_C 101.6 confirmed by HSQC which showed cross peak between δ_H 4.16 and δ_C 101.6. The downfield shift of C3 of aglycon at 74.8 (ref. 18) and the presence of a cross peak in the HMBC spectrum between δ_H 4.16 (H-1′) and δ_C 74.8 (C-3) confirmed the attached sugar at C3 of aglycon, from the value of anomeric proton and coupling constant predicted the sugar as β-glucopyranosyl confirmed by six carbon resonances were assigned for *O*-β-glucopyranosyl at δ_C 77.26, 77.13, 74.6, 70.51 and 61.53 of C-5′, 3′, 2′, 4′ and 6′ respectively.[20] Full assignments of the ^{1}H and ^{13}C NMR spectra (Fig. S9 and S10†) were consolidated using ^{1}H-^{1}H Cosy, HSQC, and HMBC experiments to confirm the compound 1 as 5(6) dihydrostigmast 22en 3-*O*-β-glucopyranoside. The molecular formula was established as $C_{35}H_{60}O_6$ from negative ESI mass spectrum (Fig. S1†) which showed the molecular ion peak at m/z 575.4502 $[M–H]^-$ to confirm the identification of metabolite 1 as 5(6) dihydrostigmast 22en 3-*O*-β-glucopyranoside (DHS) Fig. 1.

Metabolite (2). Colourless needles (12 mg) were obtained as a nonpolar substance from butanol fraction (V), R_f; 0.22 in acetate : methanol (80 : 20 v/v). It showed no fluorescence under UV light and gave a yellow color on TLC after spraying with 10–15% ethanol/H_2SO_4 after heating at 120 °C. ^{1}H NMR (850 MHz, DMSO-d6) (Table 1, Fig. S9†). Chromatographic data was expected that metabolite 2, a non-phenolic glycoside. Positive ESI-MS spectrum (Fig. S8†) exhibited a molecular ion peak at m/z 563 $[M + H]^+$ proved the corresponding molecular weight of 562

Table 1 ^{1}H and ^{13}C NMR spectrum (850 & 213 MHz, $DMSOd_6$) of metabolites (DHS and EGG)[a]

• Metabolite 1, DHS

	^{1}H NMR				^{1}H NMR		
No.	δ_H, J (Hz)	^{13}C NMR/HSQC δ_C	DEPT-135	No.	δ_H, J (Hz)	^{13}C NMR/HSQC δ_C	DEPT-135
1	1.72 (m)	33.80 (t)	CH_2	**19**	1.03 (s)	19.41 (q)	CH_3
2	1.89 (m)	29.13 (t)	CH_2	**20**	1.91 (m)	40.56 (d)	CH
3	3.96 (m)	74.8 (d)	CH	**21**	0.98 (d, 6 Hz)	21.61 (q)	CH_3
4	2.013 (m)	34.9 (t)	CH_2	**22**	5.15 (dd, 15.3, 7.6 Hz)	138.6 (d)	CH
5		45.5 (d)	CH	**23**	5.01 (dd, 15.3, 7.6 Hz)	129.2 (d)	CH
6		28.36 (t)	CH_2	**24**		30.4 (d)	CH
7		32.4 (t)	CH_2	**25**		36.06 (d)	CH
8		31.8 (d)	CH	**26**	0.88 (d, 6.8 Hz)	20.21 (q)	CH_3
9		51.05 (d)	CH	**27**	0.79 (d, 6.8 Hz)	19.06 (q)	CH_3
10	—	38.3 (Q)	C	**28**		25.36 (t)	CH_2
11		23.0 (t)	CH_2	**29**	0.78 (t, 7.7 Hz)	12.24 (q)	CH_3
12		37.7 (t)	CH_2	**1′**	4.16 (d, 7.8 Hz)	101.0 (d)	CH
13	—	42.6 (q)	C	**2′**	3.03–3.65	74.6 (d)	CH
14		56.2 (d)	CH	**3′**	Remaining sugar protons	77.13 (d)	CH
15		24.34 (t)	CH_2	**4′**		70.51 (d)	CH
16		26.01 (t)	CH_2	**5′**		77.26 (d)	CH
17		55.9 (d)	CH	**6′**		61.53 (t)	CH_2
18	0.62 (s)	12.3 (q)	CH3				

• Metabolite 2, EGG

No.	^{1}H NMR δ_H, J(Hz)	^{13}C NMR δ_C	No.	^{1}H NMR δ_H, J(Hz)	^{13}C NMR δ_C
1	—	172.88	**1′**	4.14 (1H, dd, J = 11.9, 5.1 Hz, H-1′-β) 4.35 (1H, dd, J = 11.9, 2.5 Hz, H-1′-α)	65.08
2	2.31 (2H, t, J = 7.6 Hz)	34.03	**2′**	3.77 (m, 1H, H-2′) 2.58 (1H, s, OH-2′)	74.74
3	1.49 (4H, m)	24.92	**3′**	3.89 (1H, dd, J = 11.0, 5.1 Hz, H-3′)	63.11
4	Unresolved	28.91	**1″**	4.66 (1H, d, J = 6 Hz, H-1″)	98.73
5	Unresolved	29.18	**2″**	3.17–3.42 Remaining sugar protons 4.56 (1H, d, J = 3.4 Hz, OH-3″) 4.77 (IH, d, J = 4.2 Hz, OH-4″) 5.39 (1H, d, J = 4.2 Hz, OH-2″)	72.09
6–16	1.23 [22H, brs, (CH_2)]	29.53	**3″**		70.20
17	Unresolved	29.25	**4″**		69.00
18	Unresolved	31.76	**5″**		73.37
19	1.49 (4H, m)	22.56	**6″**		173.05
20	0.853 (3H, t, J = 6.8 Hz, Me-20)	14.41			

[a] HSQC; Heteronuclear Single Quantum Coherence, DEPT-135; Distortionless Enhancement by Polarization Transfer (shows CH/CH_3 with a positive phase and CH_2 with a negative one), d, doublet, t; triplet, q; quartet, Q; quaternary, s; single.

and molecular formula $C_{29}H_{54}O_{10}$; displaying no degree of unsaturation, and so it is aliphatic open chain compound of sp^3 hybridization. All ^{1}H and ^{13}C NMR signals of the aglycone were identified by the comparison with structurally related compounds published before[21] to identify metabolite 2 aglycone as long chain fatty acid attached with glycerol, ^{1}H and ^{13}C NMR spectrums (Table 1, Fig. S9 and S10†) exhibited a triplet methylene signal at δ_H 2.31 and its corresponding carbon resonance at δ_C 34.03 assigned for C-2, multiplet methylene signal at δ_H 1.49 integrated for 4H with carbon resonance at δ_C 24.92 assigned for C-3, this was in addition to abroad singlet signal with integration of 22 protons being for 11 methylene groups at δ_H 1.23 and δ_C 29.53 assigned for C-6-16, terminated by a triplet methyl group at δ_H 0.85 (δ_C 14.41) and finally the presence of carbon resonance at δ_C 172.88 assigned for C-1 to confirm the presence of eicosanoic acid esterified by glycerol group which confirmed by the presence of oxymethin proton at $\delta\delta_H$ 3.77(1H, m) and carbon resonance at δ_C 70.20 assigned for C-2′, and two methylene groups at δ_H 4.14 (1H, dd, J = 11.9, 5.10 Hz, H-1′, β), 4.35(1H, dd, J = 11.9, 2.55 Hz, H-1′, α) and 3.89 (2H, dd, J = 11.05, 5.10 Hz, H-3′) and confirmed by corresponding carbon resonance at 65.07 and 63.10 assigned for C-1′ and 3′ respectively to confirm aglycon part as 1-*O*-eicosanoyl glycerol. Additionally, the presence of anomeric proton at δ_H 4.66(d, J = 6.00

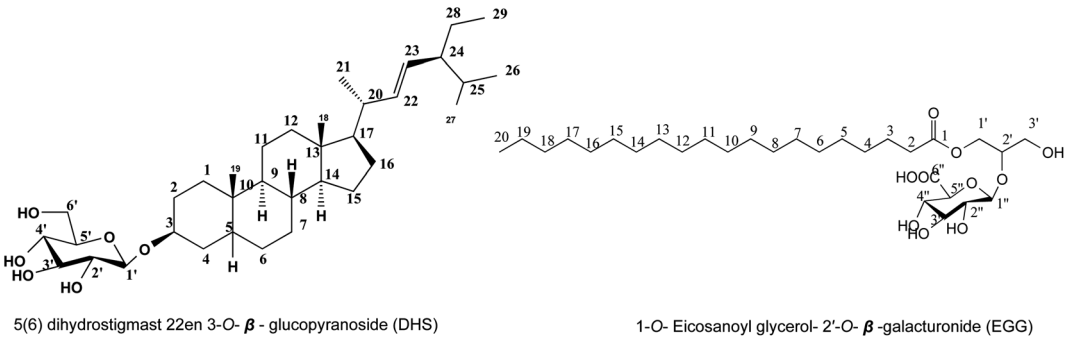

Fig. 1 The chemical structure of isolated metabolites from the *n*-butanol fraction of *H. integrifolia* (Roxb.) leaves.

Hz) was confirmed by the presence of anomeric carbon resonance at 98.7 assigned for *O*-β-hexosyl moiety, and form their δ and *J* value; the remaining protons of sugar moiety between 3.17–3.25 predicted the glycone as galacturonic confirmed by carbon resonances at 72.09, 70.20,69.00, 73.37 and 173.05 assigned for 2″, 3″, 4″, 5″ and 6″ respectively.[22] The attachment of galacturonic acid to C-2′ of glycerol was confirmed by the downfield shift of C-2′ by comparing the experiment data with those previously reported in.[21] Metabolite EGG was finally identified as 1-*O*-eicosanoyl glycerol-2′-*O*-β-galacturonide (EGG) Fig. 1.

Cell viability and cytotoxicity against vero cells

The cytotoxic effects of the *n*-butanol fraction of *H. integrifolia*, DHS, EGG, and acyclovir were assessed in Vero cells using different concentrations (1500, 1000, 500, 250, 125, 62.5, and 31.25 μg mL^{-1}) for 48 hours. The data analysis revealed dose-dependent effects, with higher activity observed at lower concentrations (Fig. 2). To ensure accurate antiviral screening, non-cytotoxic doses were selected, and the half-cytotoxic concentrations (CC_{50}) of the tested substances were determined using the MTT assay.

The half maximal cytotoxic concentration (CC_{50}) for the *n*-butanol fraction of *H. integrifolia*, DHS, and EGG, as well as the standard drug acyclovir, was assessed on Vero cells using the MTT assay (Fig. 3 and Table 2). Both the acyclovir and *n*-butanol fractions showed CC_{50} values of 283.11 ± 4.04 and 432.89 ± 2.02 μg mL^{-1}, respectively. DHS showed a CC_{50} of 1156.47 ± 3.44 μg mL^{-1}, while EGG showed a CC_{50} of 1217.09 ± 2.94 μg mL^{-1}, which indicated that both DHS and EGG had less toxicity than the *n*-butanol fraction and acyclovir against the Vero cell line. Among the tested materials the EGG has significantly ($p < 0.001$) the highest CC_{50} value followed by DHS.

Whereas the maximum non-toxic concentration (MNTC) on Vero cells was estimated to be 125, 250, 500, and 500 μg mL^{-1} for acyclovir, *n*-butanol fraction, DHS, and EGG respectively, this was used for testing the antiviral activities. The results presented those concentrations up to 500 μg mL^{-1} to both compounds DHS and EGG were more than 90% cell viability, which indicates that the sample is safe for normal cells (Table 2). Moreover, the highest value for maximum non-toxic concentration (MNTC) was achieved by the DHS and EGG indicating its relative safety on the cell lines.

The morphological characteristics of Vero cells treated with different concentrations of the tested samples

The current findings demonstrated that after treatment with the tested samples; *n*-butanol fraction of *H. integrifolia*, DHS, and EGG as well as the standard drug acyclovir; the morphology of Vero cells changed in a concentration-dependent manner. With total or partial monolayer loss, the morphological properties of Vero cells treated with various doses were changed. In

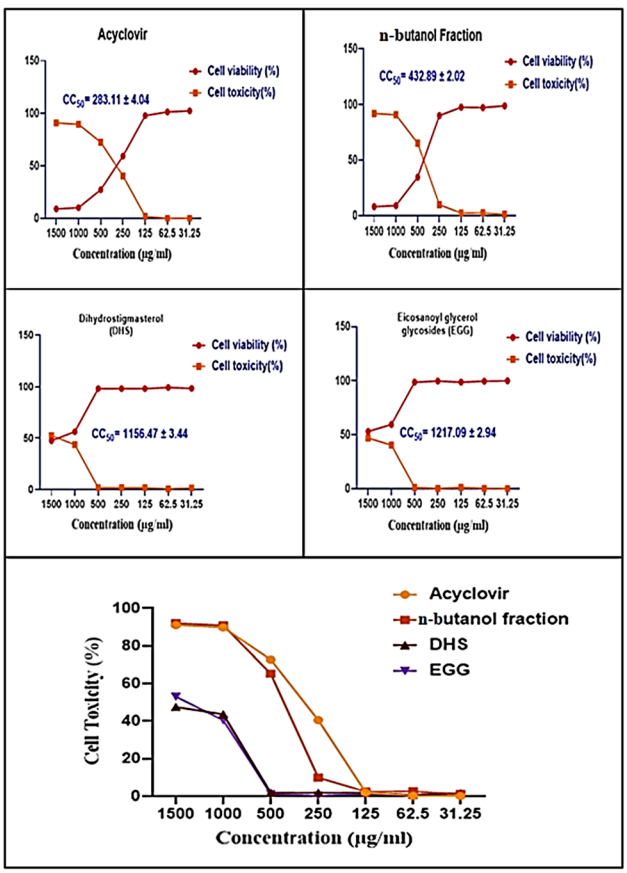

Fig. 2 Cell viability and cytotoxicity of *n*-butanol fraction of *H. integrifolia*, DHS, and EGG as well as the standard drug acyclovir against normal Vero cells at different concentrations. The CC_{50} was expressed as mean ± standard error (SE) calculated from three replicates for each level using nonlinear regression analysis by plotting log inhibitor *versus* normalized response (variable slope).

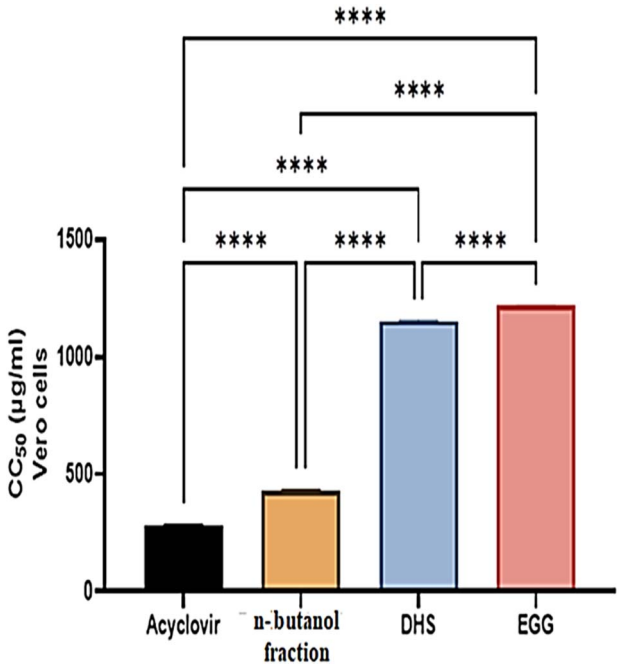

Fig. 3 The CC_{50} of *n*-butanol fraction of *H. integrifolia*, DHS, and EGG as well as the standard drugs acyclovir against normal Vero cells at different concentrations. Data were expressed as mean ± standard error (SE) calculated from three replicates for each level using one-way analysis of variance (ANOVA), Tukey post hoc test at $p < 0.05$. ns: not significant; *: significant at $p < 0.05$ level; **: significant at $p < 0.01$ level; ***: significant at $p < 0.001$ level; and ****: significant at $p < 0.0001$ level.

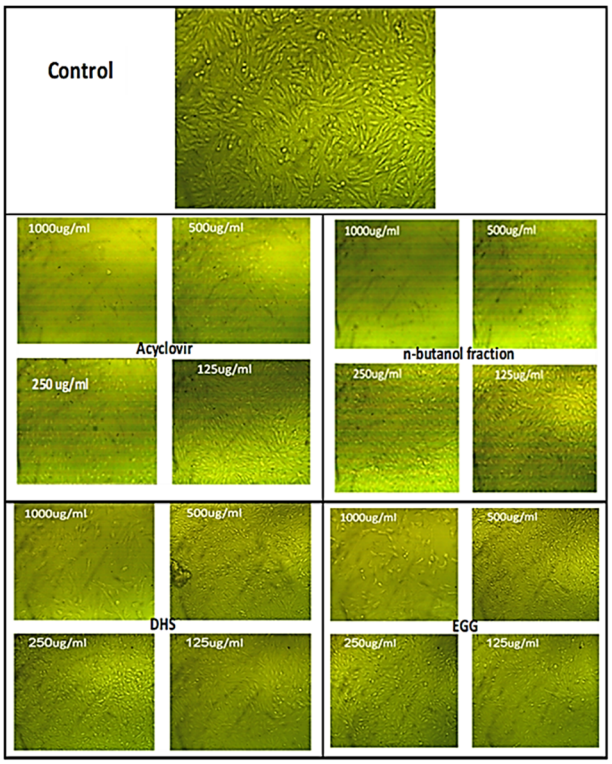

Fig. 4 The morphological characteristics of Vero cells treated with different concentrations of each sample.

comparison to untreated cells, some treated cells shrank or granulated at high concentrations. Lowering the concentrations resulted in a reduction or disappearance of these morphological alterations. Higher doses caused morphological abnormalities, such as rounding and detachment, but concentrations of 62.5 and 31.25 g mL^{-1} did not cause harm to the cell monolayer (Fig. 4).

Antiviral activity of tested samples using the MTT assay technique

The antiviral activity of the *n*-butanol fraction of *H. integrifolia*, DHS, and EGG was evaluated *versus* HSV-1 and CoxB4 virus. The antiviral activity at nontoxic concentrations and IC_{50} for each sample were identified and illustrated in (Table 2). The results of the present study revealed that EGG exhibited the highest antiviral activity against HSV-1, with an IC_{50} value of 66.96 ± 3.4 µg mL^{-1}, followed by DHS, *n*-butanol fraction, and acyclovir, with IC_{50} values of 141.81 ± 4.5, 303.72 ± 11.1, and 347.22 ± 5.7 µg mL^{-1}, respectively. Moreover, EGG also demonstrated the highest antiviral activity against CoxB4 compared to the other tested samples, with an IC_{50} value of 78.14 ± 12.8 µg mL^{-1}. On the other hand, the n-butanol fraction exhibited a non-significant antiviral activity against CoxB4, with an IC_{50} value of 305.39 ± 4.7 µg mL^{-1}. However, DHS showed a significant decrease in the IC_{50} value (171.46 ± 6.0 µg mL^{-1}) compared to acyclovir (327.05 ± 6.0 µg mL^{-1}).

Table 2 Antiviral assay of different materials showing MNTC, CC_{50}, IC_{50}, and selective indices (SIs) against HSV-I and CoxB4 viruses[a]

	MNTC (µg mL^{-1})	CC_{50} (µg mL^{-1}) ± SE	IC_{50} (µg mL^{-1}) ± SE		SI (CC_{50}/IC_{50})	
Samples	Vero cells	Vero cells	HSV-1	CoxB4	HSV-1	CoxB4
Acyclovir	125	283.11 ± 4.04	347.22 ± 5.7	327.05 ± 6.0	0.82	0.87
n-Butanol fraction	250	432.89 ± 2.02****	303.72 ± 11.1*	305.39 ± 4.7 ^{ns}	1.43	1.42
DHS	500	1156.47 ± 3.44****	141.81 ± 4.5****	171.46 ± 6.0****	8.16	6.74
EGG	500	1217.09 ± 2.94****	66.96 ± 3.4****	78.14 ± 12.8****	18.18	15.58

[a] The half maximal cytotoxic (CC_{50}) and inhibitory concentration (IC_{50}); selectivity indexes (SIs). Data were expressed as mean ± standard error (SE) calculated from three replicates for each level using one-way analysis of variance (ANOVA), Tukey *post hoc* test at $p < 0.05$. ns: non-significant; *: significant at $p < 0.05$ level; **: significant at $p < 0.01$ level; ***: significant at $p < 0.001$ level; and****: significant at $p < 0.0001$ level compared to acyclovir.

The selectivity indices (SIs) of tested samples, namely Acyclovir, *n*-butanol, DHS, and EGG, against two different viruses, HSV-1 and CoxB4 were assessed. The SIs were calculated as the ratio of the concentration required to inhibit viral replication by 50% (IC_{50}) in uninfected cells to that in infected cells. For HSV-1, the SIs were found to be 0.82, 1.43, 8.16, and 18.18 for Acyclovir, *n*-butanol, DHS, and EGG, respectively. Among these compounds, EGG showed the highest SI, indicating its potential as a selective antiviral agent against HSV-1. Similarly, for CoxB4, the SIs were found to be 0.87, 1.42, 6.74, and 15.58 for Acyclovir, *n*-butanol, DHS, and EGG, respectively. Again, EGG showed the highest SI, suggesting its potential as a selective antiviral agent against CoxB4 as well. Overall, the results indicated that EGG possesses potent antiviral activity against both HSV-1 and CoxB4 viruses. DHS also showed significant antiviral activity, particularly against HSV-1 viruses. The *n*-butanol fraction demonstrated moderate activity against HSV-1 but did not exhibit significant activity against CoxB4. Acyclovir, a commonly used antiviral drug, showed less potency compared to EGG and DHS against both viruses.

Percentage of antiviral activity and protection against HSV-I and CoxB4 viruses using the MTT assay

The antiviral effects of the tested samples against HSV-1 and CoxB4 were evaluated, and the percentages of antiviral activity and protection provided by each sample were determined. Present findings revealed that the antiviral activity percents of Acyclovir, *n*-butanol, DHS, and EGG against HSV-1, were 47.84%, 67.05%, 82.19%, and 89.94%, respectively. Similarly, the antiviral activity percent against CoxB4 of acyclovir, *n*-butanol, DHS, and EGG was 44.44%, 57.23%, 54.52%, and 66.40%, respectively. Notably, EGG exhibited the highest antiviral activity percentage among all the tested samples against both HSV-1 and CoxB4 ($p < 0.001$). Furthermore, the protection percentage provided by the tested samples was assessed against HSV-1. The protection percentages for acyclovir, *n*-butanol, DHS, and EGG were 44.54%, 58.29%, 84.24%, and 92.18%, respectively. Similarly, the protection percentages for the same tested samples against CoxB4 were 44.48%, 52.58%, 56.04%, and 68.26%, respectively. These results indicate that DHS and EGG provided significantly higher protection against both HSV-1 and CoxB4 compared to acyclovir. The *n*-butanol fraction showed non-significant differences in protection compared to acyclovir. EGG demonstrated the highest protection percentages against both viruses, suggesting its potential as an effective protective agent (Table 3).

Assessment of the cell viability of the MNTC of tested samples on HSV-1 and CoxB4

Table 4 displays the viability of two viruses, HSV-1 and CoxB4 when exposed to the maximum non-toxic concentrations of each sample. Vero cells were infected with these viruses, with and without the tested compounds, for 48 hours. An MTT assay was used to evaluate cell viability. The cell viability of control Vero, HSV-1-infected Vero cells, and HSV-1-infected Vero cells treated with Acyclovir, *n*-butanol, DHS, and EGG were determined. The results showed that the cell viability of control Vero was 99.97%. However, in the presence of HSV-1, the cell viability of Vero cells decreased significantly to 32.77%, ($p < 0.0001$). The cell viability percent of HSV-1-infected Vero cells treated with Acyclovir, *n*-butanol, DHS, and EGG were, 71.57%, 81.17%, 86.35%, and 95.63 respectively, indicating a significant increase in cell viability compared to the untreated HSV-1-infected Vero cells ($p < 0.0001$). Notably, EGG exhibited the highest cell viability percent among the tested samples, with a value of

Table 4 The viral activities in the presence or absence of each sample correspond to the control. Vero cells response to HSV-1. And response to CoxB4 virus[a]

Cell viability (%)		
	HSV-1 virus	CoxB4 virus
Control Vero	99.97 ± 0.033	100.0 ± 0.037
Virus + Vero	32.77 ± 1.73****	40.64 ± 2.80****
Acyclovir	71.57 ± 2.63**	76.55 ± 3.29**
n-Butanol fraction	81.17 ± 5.22*	81.56 ± 3.17*
DHS	86.35 ± 4.79	73.03 ± 3.75***
EGG	95.63 ± 5.044	79.83 ± 4.12**

[a] Data were expressed as mean ± standard error (SE) calculated from three replicates for each level using one-way analysis of variance (ANOVA), Tukey post hoc test at $p < 0.05$. ns: non-significant; *: significant at $p < 0.05$ level; **: significant at $p < 0.01$ level; ***: significant at $p < 0.001$ level; and****: significant at $p < 0.0001$ level compared to control vero.

Table 3 The antiviral assay of the samples and acyclovir showing antiviral activity and cell protection rate percentage (CPR%) against HSV-I and CoxB4 viruses[a]

	Antiviral activity (%)		CPR (%)	
Samples	HSV-1	CoxB4	HSV-1	CoxB4
Acyclovir	47.84 ± 2.94	44.44 ± 2.51	44.54 ± 3.06	44.48 ± 2.42
n-Butanol fraction	67.05 ± 3.43^{ns}	57.23 ± 2.51*	58.29 ± 5.17^{ns}	52.58 ± 1.53^{ns}
DHS	82.19 ± 4.42**	54.52 ± 2.8^{ns}	84.24 ± 3.74***	56.04 ± 1.50*
EGG	89.94 ± 5.71***	66.40 ± 1.82***	92.18 ± 3.79***	68.26 ± 2.82***

[a] Data were expressed as mean ± standard error (SE) calculated from three replicates for each level using one-way analysis of variance (ANOVA), Tukey *post hoc* test at $p < 0.05$. ns: non-significant; *: significant at $p < 0.05$ level; **: significant at $p < 0.01$ level; ***: significant at $p < 0.001$ level; and ****: significant at $p < 0.0001$ level compared to acyclovir.

95.63%. These results suggest that EGG has a potential protective effect against HSV-1 infection.

On the other hand, the cell viability of control Vero cells was 100.00%. While CoxB4 infected Vero cells, the cell viability was reduced by 59.36% compared to control Vero cells. However, treatment with acyclovir, *n*-butanol, DHS, and EGG resulted in increased cell viability percentage ($p < 0.001$) scored 76.55%, 81.56%, 73.03%, and 79.83%, respectively, compared to CoxB4 infected Vero cells. These results demonstrate that CoxB4 infection significantly reduced cell viability, which was partially restored by treatment with the tested samples. Notably, treatment with *n*-butanol and EGG resulted in the highest percentage increase in cell viability, indicating their potential as effective therapeutic agents for the treatment of CoxB4 infection.

Microscopic examination of HSV-1 and CoxB4 reveals antiviral activity of tested samples

The microscopic examination of HSV-1 and CoxB4 revealed irregular outlines, cytoplasmic projections, and intense cytoplasmic vacuolization, along with nuclear membrane disintegration and a mottled appearance of the cytoplasm. Additionally, a microscopic examination of control Vero, infected Vero cells, and infected Vero cells treated with acyclovir, n-butanol, DHS, and EGG was determined at MNTC, as shown in Fig. 5 and 6 findings present showed that all four samples exhibited antiviral activity against both HSV-1 and CoxB4 viruses. Specifically, a reduction in the cytopathic effect caused by the viruses in the presence of the compounds was observed, including a decrease in cytoplasmic vacuolization, nuclear membrane disintegration, and a mottled appearance of the cytoplasm. Notably, EGG demonstrated the most significant antiviral activity against both HSV-1 and CoxB4 viruses, as evidenced by the highest reduction in cytopathic effect compared to the other tested compounds.

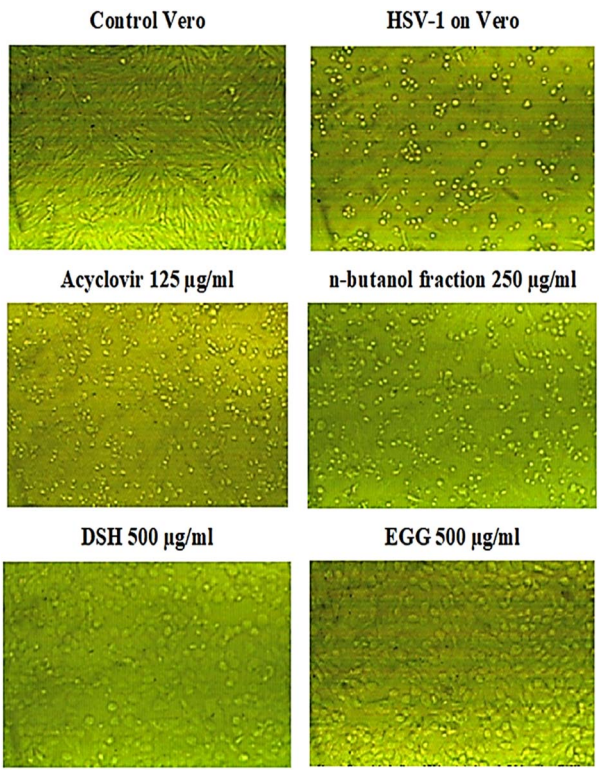

Fig. 5 Microscopical examination of tested samples at MNTC on infected Vero cells with HSV-1 virus.

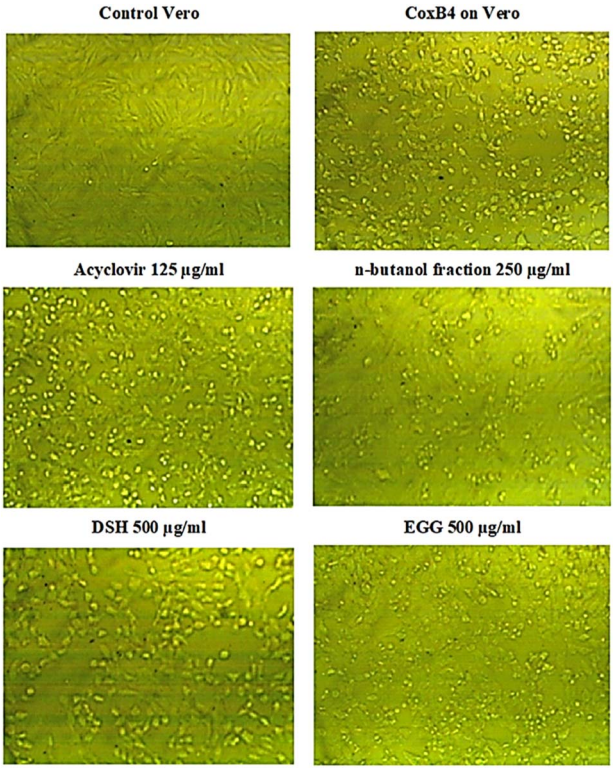

Fig. 6 Microscopical examination of tested materials at MNTC on infected VERO cells with CoxB4 virus.

Evaluation of antimicrobial activity

Screening of the potential antimicrobial activity (MIC) of *H. integrifolia* *n*-butanol fraction, DHS, and EGG against some MDR microorganisms *in vitro* was done using an XTT assay. All examined drug-resistant microbial strains were cultured overnight at 37 °C in Brain Heart Infusion (BHI) Broth to determine the inhibitory percentage at 3.9 µg mL^{-1}, and MIC of the tested samples against drug-resistant strains. The DHS and EGG exerted the highest inhibition percentages with low MIC Table 6 compared to *n*-butanol fraction against MRSA, ESBL-*Escherichia coli*, Carbapenem-resistant *Klebsiella pneumonia*, and Fluconazole-resistant *Candida albicans*. DHS; afforded the highest inhibition potency against all tested resistant strains (Table 5), with 100% inhibition of the growth of MRSA as well as Carbapenem-resistant *Klebsiella pneumonia*, 91.08% inhibition against Fluconazole-resistant *Candida albicans*, 71.35% inhibition against ESBL-*Escherichia coli*, and zero % inhibition against Vancomycin-resistant *Enterococcus faecalis*. In addition, EGG; showed high inhibition potency against all tested resistant strains with 85% inhibition of the growth of MRSA as well as

Table 5 Mean of inhibitory percentages (%) of samples at 3.9 μg mL^{-1} against microbial strains

	n-Butanol fraction	DHS	EGG
MDR-microorganisms	Mean of inhibitory percentages (%) ±SD		
• Gram-positive bacteria			
Methicillin-resistant *Staphylococcus aureus* (MRSA) ATCC-700788	62.17 ± 1.3	100 ± 0.00	86.69 ± 2.2
Vancomycin-resistant *Enterococcus faecalis* ATCC-BAA-2365	0	0	0
• Gram-negative bacteria			
ESBL-*Escherichia coli* ATCC-BAA-199	29.74 ± 0.58	71.35 ± 1.1	56.19 ± 0.58
Carbapenem-resistant *Klebsiella pneumonia* ATCC- BAA-2342	72.16 ± 0.73	100 ± 0.00	84.31 ± 1.7
• Fungi			
Fluconazole- resistant *Candida albicans* ATCC-MYA-1003	61.25 ± 1.1	91.08 ± 0.74	71.92 ± 1.9

Carbapenem-resistant *Klebsiella pneumonia*, 71.92% inhibition against Fluconazole-resistant *Candida albicans* and 56.19% inhibition against ESBL-*Escherichia coli* but it showed zero % inhibition against Vancomycin-resistant *Enterococcus faecalis*.

In silico molecular docking study

To scout for potential targets affected by the isolated compounds of *H. integrifolia* and their antiviral activity against the HSV-1 virus, molecular docking simulations were performed *in silico* with DNA polymerase (DNA-POL). DNA-POL is a vital enzyme in the replication cycle of herpes viruses and is the primary target for many antiviral drugs.[23] Traditional treatments for herpes viral infections have focused on targeting DNA-POL, which has been highly effective. However, the emergence of drug-resistant strains, particularly in newborns and immunocompromised individuals, underscores the need for continued development of antiviral medications against herpes.[24] Furthermore, DNA gyrase is a type II topoisomerase that uses ATP hydrolysis to introduce negative supercoiling into DNA. It plays a crucial role in bacterial cellular processes and is absent in higher eukaryotes, making it an attractive target for antibacterial drugs.[25] The goal of this research's docking study is to identify potential binding interactions of the two most active hits, DHS, and EGG on two vital viral and bacterial enzymes. Acyclovir's binding mode demonstrated two hydrogen bond interactions with the highly conserved residues (Lys811, Asn815) located in the binding cleft, effectively blocking viral DNA replication. This was associated with a binding energy of −6.522 kcal mol^{-1}. DHS displayed a high binding affinity, forming four hydrogen bonds with the key residues of the active site (Lys811, Cys814, Asn815, and Ser720), and had a docking score value of −7.172 kcal mol^{-1}. On the other hand, EGG established only two hydrogen bonds with Ala719 and Ser720, resulting in a binding energy of −5.776 kcal mol^{-1}. Additionally, notable hydrophobic interactions were observed with Arg785, Lys786, and Glu925 residues (Fig. 7, Table S1†).

The co-crystallized ligand (Ciprofloxacin), showed that the binding score was −8.242 kcal mol^{-1}. Moreover, two hydrogen bond interactions with Arg1033 and His1081 were observed, and the co-crystallized ligand displayed hydrophobic interactions within the binding region with Asp510, Tyr580, and Tyr1150 residues. Focusing on DHS, it demonstrated docking

Table 6 The minimal inhibitory concentrations (MIC_S) of the tested samples required for inhibiting 100% of the tested microorganisms

	n-Butanol fraction	DHS	EGG
MDR microorganisms	MIC (μg mL^{-1})		
• Gram-positive bacteria			
Methicillin-resistant *Staphylococcus aureus* (MRSA) ATC -700788	15.63	3.9	7.81
Vancomycin-resistant *Enterococcus faecalis* ATCC-BAA-2365	0	0	0
• Gram-negative bacteria			
ESBL-*Escherichia coli* ATCC-BAA-199	62.5	15.63	31.25
Carbapenem-resistant *Klebsiella pneumonia* ATCC – BAA-2342	15.63	3.9	15.63
• Fungi			
Fluconazole- resistant *Candida albicans* ATCC-MYA-1003	31.25	7.81	15.63

score = −7.642 kcal mol^{-1} and strong DNA gyrase inhibitory action, where the oxygen atom of the O–H group is bound to Asp510 whereas His1081 is shared *via* C–H interaction.

Besides, hydrophobic interactions were observed with the amino acids Tyr580, Lys581, Tyr1150, Asp1151, and Asn1153. The inhibitory activity is identified by both the docking score and the

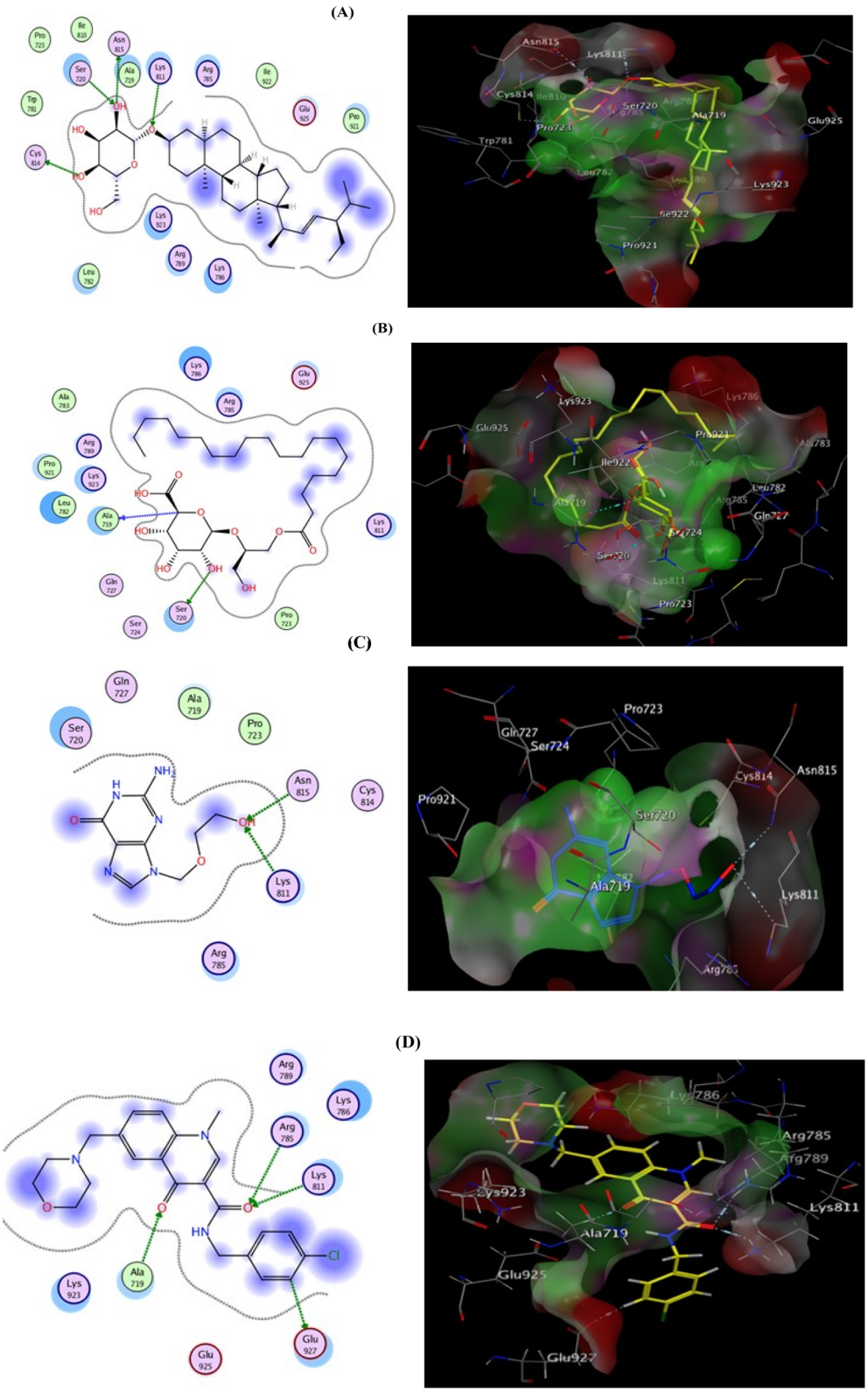

Fig. 7 2D (left) and 3D (right) proposed interactions of DHS (A), EGG (B), Acyclovir (C), and ligand (D) inside the DNA polymerase active binding site.

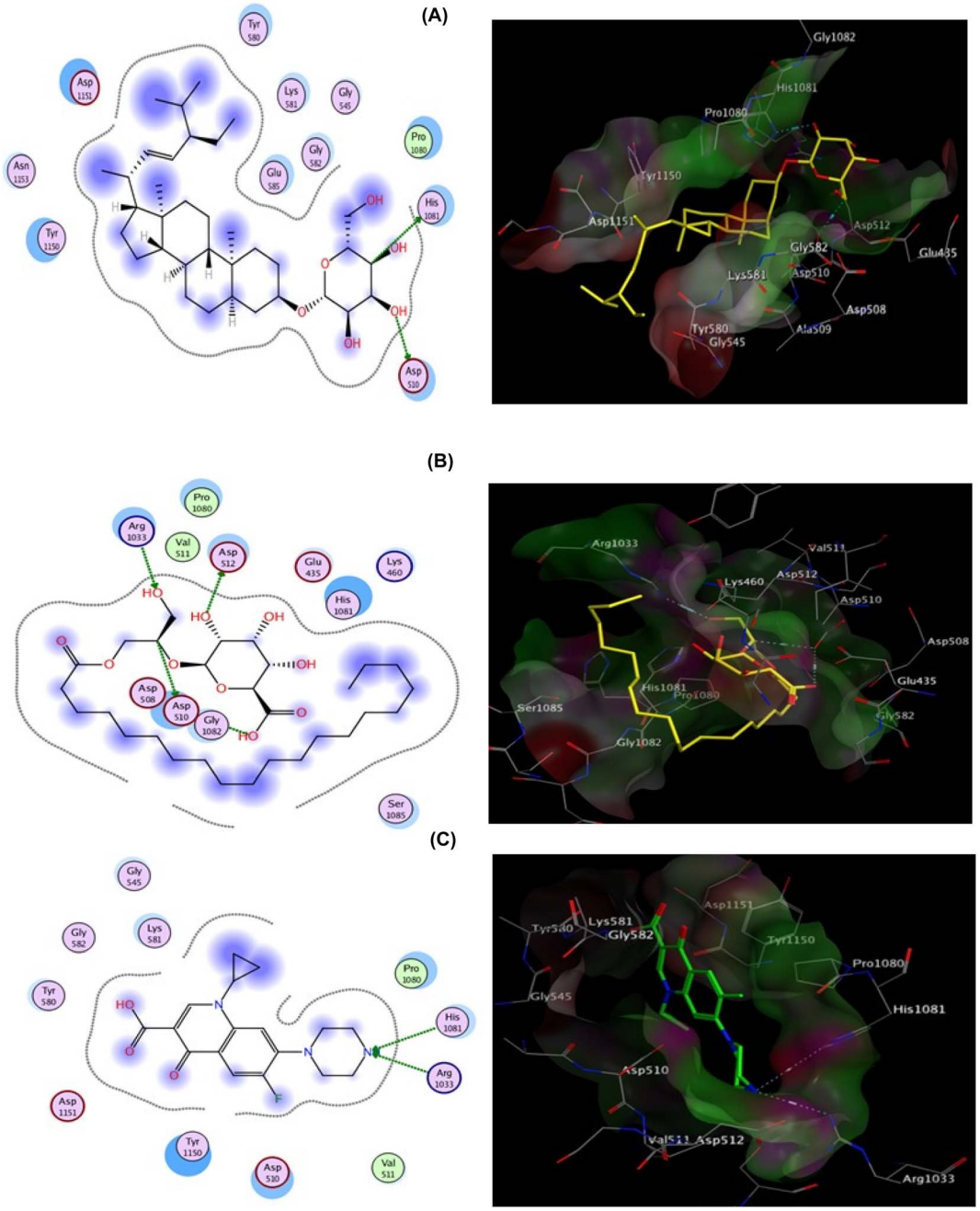

Fig. 8 2D (left) and 3D (right) proposed interactions of DHS (A), EGG (B), and Ciprofloxacin (C) inside the DNA gyrase active binding site.

binding pose which may be explained by the fact that the most active compound was able to interact with the critical residues in the active site. EGG was able to fit inside the active site forming four hydrogen bonds *via* binding with four important residues: Asp510, Asp512, Arg1033, and the co-crystallized ligand, confirming the MIC values recorded for both hits (Fig. 8, Table S2†)., and Gly1082. However binding energy was −4.561 kcal mol^{-1} lower than both DHS. The docking scores and bioavailability scores suggest that DHS would have higher binding activity and potentially better drug-like properties compared to EGG. However, the *in vitro* antiviral activity results for HSV1 and COXB4 indicated that EGG has the highest antiviral activity, as evidenced by the lowest IC_{50} value, the highest selectivity index (SI) value, and the highest protection rate. This observation can be attributed to the fact that docking studies offer valuable insights into the potential binding modes and affinities of compounds to a target protein. However, they are not always precise in predicting the actual biological activity of compounds. Experimental results provide a comprehensive understanding of the compounds' impact on viral replication within a cellular context, considering additional factors beyond binding affinity. These factors include compound stability, metabolism, cellular uptake, and target specificity, which collectively contribute to the overall effectiveness of the compounds.[26,27] A previous study has

documented that glycerol derivatives have demonstrated antiviral activity against various enveloped viruses, including HSV-1.[28] However, the study did not reveal any inhibitory effect on nonenveloped viruses. This suggests that the antiviral activity of glycerol derivatives may be linked to their ability to directly interfere with the viral envelope, causing modulatory changes that prevent the virus from binding to the host cell membrane. Furthermore, they may also inhibit RNA synthesis and viral maturation processes.[29] The antiviral activity of a compound can be highly dependent on the specific target virus or pathway.[30] EGG may possess specific properties or mechanisms that render it particularly effective against HSV-1 and COXB4, despite its lower docking score and bioavailability scores. This underscores the complexity of drug discovery and emphasizes the requirement for experimental validation and consideration of multiple factors beyond docking and bioavailability scores. Consequently, further studies, encompassing additional assays or *in vivo* models, are necessary to validate the antiviral activity of EGG and elucidate its mechanism of action.

In silico pharmacokinetics, drug-likeness, and medicinal chemistry properties

The prediction of physicochemical, ADME, pharmacokinetics, drug-likeness, and medicinal chemistry friendliness properties of metabolites present in *n*-butanol fraction of *H. integrifolia* leaves, by SwissADME tool.[31] The two metabolites, DHS and EGG, exhibited promising ADME properties with few exceptions. They were predicted to have favorable physiochemical features, including Topological Polar Surface Area, log *P* values, log *S*, bioavailability, and log K_p values. Both metabolites violated one of Lipinski's rules for oral drugs (MM > 500) but remained orally bioavailable. DHS had higher cell membrane permeability and bioavailability than EGG, as well as rotatable bonds indicating molecular flexibility. DHS also had higher gastrointestinal absorption than EGG. Both metabolites did not permeate the blood–brain barrier and were poor substrates for P-glycoprotein, ensuring low to no CNS side effects. Both metabolites were found to have high bioavailability scores.

Experimental

Plant materials

Indian Elm leaves were collected as mentioned by Mahrous, *et al.*, 2021.[32]

Extraction, fractionation, chromatographic isolation

H. integrifolia (Roxb.) Planch leaves air-dried powdered (1 kg), was extracted using 70% aq. MeOH (5 × 3 L), evaporate of aq. MeOH under vacuum dry total extract (380 g), Fractionated using different solvents; petroleum ether (3 × 250 mL), methylene chloride (4 × 250 mL), ethyl acetate (7 × 500 mL), *n*-butanol (9 × 500 mL), to yield, 6, 9, 11, and 80 g, respectively.[14,16] Fraction of *n*-butanol (80 g); applied on a silica column using methylene chloride, then methylene chloride/methanol, up to 100% methanol; using TLC/15% ethanol/H_2SO_4 at 120 °C, obtained 10 collective fractions (I–XI). To isolate three pure components, fractions III and V were applied to silica columns in sequence using ethyl acetate, ethyl acetate/methanol, and 100% methanol. Fractions III and V were applied to consecutive silica columns using ethyl acetate, then ethyl acetate/methanol, up to 100% methanol, to isolate two metabolites.

Cell culture and viruses

African green monkey kidney-derived Vero cells (CCL-81; American Type Culture Collection, USA) maintained in MEM supplemented with fetal calf serum (FCS; 10% v/v), L-glutamine (2 nM), penicillin (100 U mL^{-1}), and streptomycin (100 μg mL^{-1}) were used for the antiviral assays. Propagation of cells for up to 4 weeks, then the cells were incubated in a 5% CO_2 humidified atmosphere at 37 °C as cell line stock.[33] Herpes simplex type-1 (HSV-1), and Coxsackie B virus type 4 (COXB4) were kindly provided by the Laboratory of Virology, Microbiology Department, Faculty of Medicine (for Girls), Al-Azhar University, Cairo, Egypt.

Preparation of virus stock

Each virus was propagated in Vero cells by infecting a confluent Vero cell monolayer in 75 cm^2 culture flasks and allowed to be adsorbed for 1 h. Non-adherent particles were washed off using 2% MEM, and the infected cells were overlaid with 20 mL of 2% MEM (maintenance medium) and incubated until a full cytopathogenic effect (CPE) was observed daily for up to 4–6 days. This step was repeated twice, and then the challenge dose of each virus was determined by using plaque formation assays[34,35] and each virus harvest was stored at −20 °C until use.

Cytotoxicity assay

The maximum nontoxic concentration (MNTC) of each extract was determined by 10-fold dilutions of the different plant extracts in MEM with FCS, starting from 100 mg mL^{-1} until a 10^{-6} dilution. Then, 0.2 mL of each dilution was used to treat confluent Vero cells in four wells in a 96-well plate (Falcon; Corning, USA), and two rows were left as the control. Acyclovir (Sigma-Aldrich, St. Louis, MO, USA) was dissolved in distilled water and MNTC was also evaluated. The plates were incubated at 37 °C. The cells were examined daily using an inverted microscope to determine the minimum concentration required to produce alterations in cell morphology. The treated Vero cells did not show any morphological differences at the MNTC compared with the control Vero cells, even after 7 days. The MTT colorimetric assay (Bio Basic Inc., Canada) was performed as described previously.[36]

Antiviral function

The least harmful concentration of the investigated samples was used to treat viruses and Vero cell cultures. Virus pretreatment: exposing the viruses to the extract for an hour at 37 °C, then adding the mixture (100 μL) to the cells cultivated on a microtiter plate to test the extract's virucidal activity. The formazan absorbance values in an MTT experiment were used to compare the viability of infected and uninfected cells. The concentration needed to inhibit viral growth by 50% is known

as the IC_{50}. The ratio of the 50% antiviral concentration (IC_{50}) to the selectivity index (SI) is equal to CC_{50}/IC_{50}. Three determinations' means were computed.[37]

MTT assay protocol

The MTT assay protocol was used to evaluate the antiviral activity. This assay employed a mixed treatment approach to test the inactivation of virus particles in a virus suspension by the tested samples. The procedure involved incubating the virus suspension with non-lethal concentrations of the samples (at a 1 : 1 volume ratio) at room temperature for 1 hour. Vero cells were seeded in a 96-well plate at a density of 1×10^4 cells per well in 200 μL of media, leaving three wells empty for blank controls. The plate was then incubated overnight at 37 °C to allow the cells to attach to the wells. Next, 100 μL of the viral/sample suspension was added to the wells and mixed on a shaker at 150 rpm for 5 minutes. After incubating for one day, 20 μL of MTT solution (5 mg mL^{-1} in PBS) was added to each well. The mixture was further incubated for 5 hours to allow the conversion of MTT to formazan crystals. Subsequently, 200 μL of DMSO was added to dissolve the crystals, and the optical density (OD) was measured at 560 nm, which directly correlates with the number of cells present. All tests were compared to the standard antiviral drug Acyclovir. The percent protection was calculated using the formula $[(A - B)/(C - B)] \times 100$, where A, B, and C represent the OD560 values of the treated infected, untreated infected, and untreated uninfected cells, respectively. The IC_{50}, which indicates the concentration of the samples required to inactivate 50% of the virus particles compared to the untreated control, was determined from dose-response curves.[38]

The selectivity index (SI) is calculated

After dividing the half maximal inhibitory concentration of normal Vero cells, CC_{50}, by the specific IC_{50} of cancer cells and virally infected cells, selectivity indices (SI) were calculated. Utilising selectivity indices, which are high (SI) to signify high potency and low cellular toxicity, researchers can assess cytotoxic potential and antiviral activity in relation to the typical toxicity of cells.[39]

Determination of the cell viabilities and cell protection rate (CPR) of tested materials against Vero cells infected with viruses

Upon treatment of the cells with tested samples at their MNTCs, the cell viability of Vero cells infected with viruses was calculated using the following equation.[40]

Using the following equation, the maximum non-toxic concentration (MNTC) of the tested samples in Vero cells infected with the HSV-1 and COXB4 viruses was used to calculate the cell protection rate (CPR), or the protection provided to the cells by the test samples.[41]

Microorganisms

Methicillin-resistant *Staphylococcus aureus* (MRSA) ATCC-700788 strain is a Gram-positive strain, which was confirmed by the American Type Culture Collection to carry the mecA gene, SCCmec Type II conferring resistance to methicillin antibiotics. The strain is a Beta-lactams and MLSB inducible-resistant strain. The strain is resistant to Cefoxitin, Benzylpenicillin, Oxacillin, Imipenem, Erythromycin, Clindamycin, and Trimethoprim/Sulfamethoxazole.

Vancomycin-resistant *Enterococcus faecalis* BAA-2365 is a Gram-positive strain, which was confirmed by the American Type Culture Collection to carry the vanB, deliberating resistance to Vancomycin antibiotics.

Carbapenem-resistant *Klebsiella pneumonia* ATCC BAA-2342 strain is a Gram-negative strain, which was confirmed by the American Type Culture Collection to carry the blaKPC gene conferring resistance to carbapenem antibiotics. The strain is a Beta-lactams, resistant carbapenems, ESBL, carbapenemase Kpc strain. The strain demonstrates multidrug resistance to Temocillin, Ampicillin, Amoxicillin/Clavulanic Acid, Piperacillin, Piperacillin/Tazobactam, Cefalotin, Cefuroxime, Cefotaxime, Ceftazidime, Ceftriaxone, Cefepime, Ertapenem, Meropenem, Tobramycin, and Trimethoprim/Sulfamethoxazole.

Extended-spectrum Beta-lactamase *Escherichia coli* BAA-199 strain is a Gram-negative strain, which was confirmed by the American Type Culture Collection to belong to SHV-3-ESBL class, which has ESBL enzymes, conferring resistance to extended-spectrum cephalosporins and monobactams.

Fluconazole-resistant *Candida albicans* ATCC-MYA-1003A strain is a unicellular fungus, which confirmed by the American Type Culture Collection to be resistant against fluconazole, anidulafungin, voriconazole, and itraconazole. All organisms were obtained from the Regional Centre for Mycology and Biotechnology (RCMB) antimicrobial unit test organisms.

XTT assay

The calorimetric broth microdilution method using the XTT [2,3-bis(2-methoxy-4-nitro-5-sulfo-phenyl)-2*H*-tetrazolium-5carboxanilide] reduction assay with minor modifications was used to determine the inhibitory percentages, minimum inhibitory concentration 50 (MIC_{50}), and minimum inhibitory concentration (MIC) of the tested samples against drug-resistant strains. All microbial strains were cultured overnight at 37 °C in Brain Heart Infusion (BHI) (Oxoid, UK). XTT (Sigma) was prepared in a saturated solution at 0.5 g L^{-1} in Ringer's lactate. The solution was sterilized through a 0.22 μm-pore-size filter. The samples were serially diluted in DMSO, and 50 μL of each dilution at final concentrations of 1000–0.24 μg mL^{-1} were added to the wells of a Microtiter plate (96 wells) containing 100 μL TSB. Fifty microliters of adjusted microbial inoculum (10^6 CFU mL^{-1}) were added to each well, followed by the incubation of the Microtiter plates in the dark at 37 °C for 24 h. Subsequently, 100 μL of freshly prepared XTT was added and the plates were incubated again for 1 h at 37 °C. Calorimetric variation in the XTT assay was measured using a Microtiter plate reader (BioTECK, USA) at 492 nm. Inhibition-mediated reduction of microbial viability at 1.95 μg mL^{-1} was calculated by the following formula: % of inhibition = [1 − (ODt/

ODc)] × 100, where ODt is the mean optical density of the wells treated with the tested sample and ODc is the mean optical density of untreated wells.[42] The MIC was specified as the sample concentration that produced a 100% decrease in optical density compared with control growth results.

In silico molecular docking study

The software used in this work is the molecular operating environment (MOE-2014).[43] Concerning the antiviral activity, the new hits were docked inside the active binding site of the DNA polymerase enzyme to predict and score the poses of the protein–ligand binding using the structure of the HSV-1 POL (PDB ID: 7LUF) downloaded from the protein data bank.[44] The first redocking of the co-crystallized ligand was carried out for validation. It showed a docking score value of −6.982 kcal mol^{-1} with a root-mean-square deviation (RMSD) value of 1.07 Å. Additionally, three hydrogen bond interactions with Ala719, Arg785, and Lys811 were observed, besides, C–H interaction with Glu927. Taking into consideration their notable MIC values and anticipated interactions with *S. aureus* DNA gyrase. From the protein data bank, the crystal structure of *S. aureus* DNA gyrase complexed with ciprofloxacin inhibitor (PDB: 2XCT) was downloaded.[45] The co-crystallized ligand (Ciprofloxacin) is first re-docked with the DNA gyrase enzyme for validation. It showed RMSD = 0.27 and maintained its orientation, demonstrating the effectiveness of the docking approach used.

Prediction of physicochemical, ADME pharmacokinetics, drug-likeness, and medicinal chemistry properties

The absorption, distribution, metabolism, and elimination (ADME) properties of metabolites were probed using SwissADME.[31] The physicochemical properties, lipophilicity, water-solubility, pharmacokinetics, drug-likeness, and medicinal chemistry of the phytochemicals were evaluated using various parameters.[46,47] For the computational simulation, canonical SMILES of the selected 206 phytochemicals were obtained from the PubChem database[48] and incorporated into the SwissADME tool for the prediction of the properties.

Statistical analysis

The half-maximal inhibitory concentration (IC_{50}) and the half-maximal cytotoxic concentration (CC_{50}) were calculated using GraphPad Prism version 9.5.1. The level of significance was set at ($p < 0.05$) using nonlinear regression analysis by plotting log inhibitor *versus* normalized response (variable slope). The mean and standard error (SE), computed from three replicates for each level, was used to express quantitative data. The one-way analysis of variance (ANOVA) and Tukey *post hoc* test were used to make various comparisons.

Conclusion

The tree *H. integrifolia* has a substantial percentage of biologically active substances that need to be isolated and clinically correlated for their unidentified therapeutic potential. This could provide critical baseline information for future clinical applications of the investigated drugs in HSV-1, COX-B4, and MDR phenotype protection. Based on the results of the cytotoxicity test, EGG shows potent suppression of viral infection in a dose-dependent manner while exhibiting minimal cytotoxicity to Vero cells at the highest tested concentration. The compound has a higher efficacy against HSV-1 compared to the Cox-B4 virus, as indicated by the calculated SI values. These findings suggest that EGG has potential as a therapeutic agent for combating viral infections, particularly against HSV-1. Additionally, this study explored the potential antibacterial activity of both DHS and EGG. A potent metabolite must reach its target in sufficient quantity and remain in a bioactive form long enough for the predicted biological activities to be helpful as a medicine. So, ADME is a step in the drug development process, that revealed that DHS has higher GI absorption than EGG, even though the two are non-substrates for both P-gp (P-glycoprotein).

So, ADME is a step in the drug development process, that revealed that DHS has CYP (Cytochrome P-450 isoenzymes). All the metabolites comply with the Lipinski rule of 5, with one violation (MW > 500), suggesting that the metabolites possess good drug-likeness properties upon administration. Furthermore, DHS follows the Veber rule and indicates greater bioavailability and intestinal absorption than EGG. Finally, Swiss EDME tools give valuable baseline data for future clinical trials of the researched medications in HSV-1, COX-4, and MDR phenotypic protection.

Data availability

The authors confirm that the data supporting the study's conclusions are included in the article. Supplementary materials contain raw data.

Author contribution

All authors contributed to the study's conception and design. Material preparation, data collection, and analysis were performed by all authors. All authors participated in the writing of the manuscript. All authors read and approved the final manuscript.

Conflicts of interest

The authors certify that this publication does not include any conflicts of interest. The authors declare that they have no known competing financial interests or personal relationships that could have appeared to influence the work reported in this paper.

References

1 K. K. Bhutani and V. M. Gohil, *Indian J. Exp. Biol.*, 2010, **48**, 199–207.
2 N. Kishore, D. Twilley, A. Blom van Staden, P. Verma, B. Singh, G. Cardinali, D. Kovacs, M. Picardo, V. Kumar and N. Lall, *J. Nat. Prod.*, 2018, **81**, 49–56.

3 P. Kumar Verma, M. Bala, N. Kumar and B. Singh, *Curr. Top. Med. Chem.*, 2012, **12**, 1422–1435.
4 C. Veeresham, *J. Adv. Pharm. Technol. Res.*, 2012, **3**, 200–201.
5 P. Prajapati and N. M. Patel, *Int. J. Pharma Sci.*, 2010, **1**, 34–40.
6 S. Khalid, G. Rizwan, H. Yasin, R. Perveen and H. Abrar, *Holoptelea integrifolia*, 2013, **2**, 1–4.
7 B. J. R. Kumar P and C. P. Kiladi, *Ethnobotanical Leaflets*, 2009, **10**, 3.
8 R. F. Chandler and S. N. Hooper, *Phytochemistry*, 1979, **18**, 711–724.
9 R. P. Rastogi and B. Mehrotra, *Compendium of Indian medicinal plants*, Central Drug Research Institute, 1990, 4, pp. 118–122.
10 V. Singh and Z. A. ALI, *Fitoterapia (Milano)*, 1994, **65**, 68–74.
11 V. L. Challinor and J. J. De Voss, *Nat. Prod. Rep.*, 2013, **30**, 429–454.
12 C. C. Akoh, *Food lipids: chemistry, nutrition, and biotechnology*, CRC press, 2017, 1, pp. 71–75.
13 J. A. Jackman, A. Hakobyan, H. Zakaryan and C. C. Elrod, *J. Anim. Sci. Biotechnol.*, 2020, **11**, 1–10.
14 G. N. Anyasor, O. Funmilayo, O. Odutola, A. Olugbenga and E. M. Oboutor, *J. Intercult. Ethnopharmacol.*, 2014, **3**, 78.
15 M. Bala, K. Pratap, P. K. Verma, B. Singh and Y. Padwad, *J. Ethnopharmacol.*, 2015, **175**, 131–137.
16 M. Sunil, V. Sunitha, A. Ashitha, S. Neethu, S. J. Midhun, E. Radhakrishnan and M. Jyothis, *J. Food Drug Anal.*, 2019, **27**, 195–207.
17 C. L.-T. Chang, H.-K. Kuo, S.-L. Chang, Y.-M. Chiang, T.-H. Lee, W.-M. Wu, L.-F. Shyur and W.-C. Yang, *J. Biomed. Sci.*, 2005, **12**, 79–89.
18 V. M. Sari, D. Harneti, N. Indrayati, M. N. Azmi and U. Supratman, *J. Phys.: Conf. Ser.*, 2020, **1494**(1), 012025.
19 J.-M. C. Cayme and C. Y. Ragasa, *Kimika*, 2004, **20**, 5–12.
20 P. Koli, S. Singh, B. K. Bhadoria, M. Agarwal, S. Lata and Y. Ren, *Molecules*, 2022, **27**, 5153.
21 E. Hernández-García, A. García, F. G. Avalos-Alanís, V. M. Rivas-Galindo, C. Delgadillo-Puga and M. del Rayo Camacho-Corona, *Data Brief*, 2019, **22**, 255–268.
22 M. Luisa, D. Ramos, M. Madalena, M. Caldeira and V. M. Gil, *Carbohydr. Res.*, 1996, **286**, 1–15.
23 J. Piret and G. Boivin, in *The Enzymes*, Elsevier, 2021, 50, pp. 79–132.
24 S. K. Weller and R. D. Kuchta, *Expert Opin. Ther. Targets*, 2013, **17**, 1119–1132.
25 F. Collin, S. Karkare and A. Maxwell, *Appl. Microbiol. Biotechnol.*, 2011, **92**, 479–497.
26 S. Einav, D. Gerber, P. D. Bryson, E. H. Sklan, M. Elazar, S. J. Maerkl, J. S. Glenn and S. R. Quake, *Nat. Biotechnol.*, 2008, **26**, 1019.
27 C. Fu, L. Yu, Y. Miao, X. Liu, Z. Yu and M. Wei, *Acta Pharm. Sin. B*, 2023, **13**, 498–516.
28 P. Singh, R. Hernandez-Rauda and O. Peña-Rodas, *Food Sci. Nutr.*, 2023, **11**, 2547–2579.
29 J. L. Welch, J. Xiang, C. M. Okeoma, P. M. Schlievert and J. T. Stapleton, *Mbio*, 2020, **11**(3), 1110–1128.
30 S. Mahajan, S. Choudhary, P. Kumar and S. Tomar, *Bioorg. Med. Chem.*, 2021, **46**, 116356.
31 A. Daina, O. Michielin and V. Zoete, *Sci. Rep.*, 2017, **7**, 42717.
32 F. S. M. Mahrous, H. Mohammed and R. Sabour, *Azhar International Journal of Pharmaceutical and Medical Sciences*, 2021, **1**, 91–101.
33 M. E. El Awady, M. A. N. Eldin, H. M. Ibrahim, M. E. Al Bahnasy and S. H. A. Aziz, *J. Appl. Pharm. Sci.*, 2019, **9**, 010–018.
34 K.-H. Chan, J. M. Peiris, S. Lam, L. Poon, K. Yuen and W. H. Seto, *Adv. Virol.*, 2011, **2011**, 1–7.
35 R. A. El-Shiekh, U. R. Abdelmohsen, H. M. Ashour and R. M. Ashour, *Antibiotics*, 2020, **9**, 756.
36 R. Samra, A. Soliman, A. Zaki, M. Hassan and A. Zaghloul, *Indian J. Sci. Technol.*, 2020, **13**, 2866–2875.
37 K. A. Mansour, M. El-Neketi, M.-F. Lahloub and A. Elbermawi, *Molecules*, 2022, **27**, 3639.
38 R. Dulbecco and M. Vogt, *J. Exp. Med.*, 1954, **99**, 167–182.
39 H. Takeuchi, M. Baba and S. Shigeta, *J. Virol. Methods*, 1991, **33**, 61–71.
40 Q. Sun, P. X. Shui, H. B. Li, S. J. Yang, M. H. Liu and S. J. Zhang, *Bangladesh J. Pharmacol.*, 2012, **7**, 145–149.
41 A. M. M. Youssef, Z. A. S. EL-Swaify, D. A. Maaty and M. M. Youssef, *Vitae*, 2021, **28**, e7.
42 H. A. Abuelizz, M. Marzouk, A. Bakhiet, M. M. Abdel-Aziz, E. Ezzeldin, H. Rashid and R. Al-Salahi, *Microb. Pathog.*, 2021, **160**, 105157.
43 J. K. Maier and P. Labute, *Proteins: Struct., Funct., Bioinf.*, 2014, **82**, 1599–1610.
44 R. P. Hayes, M. R. Heo, M. Mason, J. Reid, C. Burlein, K. A. Armacost, D. M. Tellers, I. Raheem, A. W. Shaw and E. Murray, *Nat. Commun.*, 2021, **12**, 3040.
45 N. S. Naik, L. A. Shastri, S. D. Joshi, S. R. Dixit, B. M. Chougala, S. Samundeeswari, M. Holiyachi, F. Shaikh, J. Madar and R. Kulkarni, *Bioorg. Med. Chem.*, 2017, **25**, 1413–1422.
46 F. Cheng, W. Li, Y. Zhou, J. Shen, Z. Wu, G. Liu, P. W. Lee and Y. Tang, *J. Chem. Inf. Model.*, 2012, **52**, 3099–3105.
47 D. E. Pires, T. L. Blundell and D. B. Ascher, *J. Med. Chem.*, 2015, **58**, 4066–4072.
48 P. R. Bhatt and R. R. Bhatt, Corporate Governance, *Int. J. Bus. Soc.*, 2017, **5**, 896–912.